

Adaptive Outlier Detection for Power MOSFETs Based on Gaussian Process Regression

Kyohei Shimozato[§] Michihiro Shintani[†], and Takashi Sato[§]

[§] Graduate School of Informatics, Kyoto University Yoshida-hon-machi, Sakyo, Kyoto 606-8501, Japan

[†] Graduate School of Science and Technology, Nara Institute of Science and Technology
8916-5 Takayama-cho, Ikoma, Nara 630-0192, Japan

Phone: +81-75-753-4801 E-mail: paper@easter.kuee.kyoto-u.ac.jp

Abstract—Outlier detection of semiconductor devices is important since manufacturing variation is inherently inevitable. In order to properly detect outliers, it is necessary to consider the discrepancy from underlying trend. Conventional methods are insufficient as they cannot track spatial changes of the trend. This study proposes an adaptive outlier detection using Gaussian process regression (GPR) with Student-t likelihood, which captures a gradual spatial change of characteristic variation. According to the credible interval of the GPR posterior distribution, the devices having excessively large deviations against the underlying trend are detected. The proposed methodology is validated by the experiments using a commercial SiC wafer and simulation.

Keywords—Outlier detection, characteristic variation, Gaussian process regression

I. INTRODUCTION

Power devices, such as SiC MOSFETs, are the important components for building efficient converters. Semiconductor devices are subject to characteristic variations, and power devices are no exception. Typically, the characteristic variation of a chip on a wafer is known to be separated into two: an underlying trend and a random noise added to it [1]. Therefore, the proper modeling of fundamental trends and the decomposition of these components are important for detecting outliers and improving manufacturing process.

SiC wafers are commonly manufactured using physical vapor transport (PVT) crystal growth. In the PVT method, wafers are grown in a heated crucible, so the basal plane bending and crystallographic dislocations due to temperature gradients are unavoidable. This heterogeneity is considered as the cause of the spatial variation of the characteristics [2], [3], [4]. In addition, bulk micro-defects can be formed randomly. Numerous studies have reported that such random defects can pose a reliability risk [5], [6], thus chips that may contain these defects must be judged as outliers. Chips with excessively large deviation from the spatial trend are likely to contain such defects because these random defects have a significant impact on the characteristic degradation.

In practice, it is difficult to detect these anomalies using conventional methods. Among others, the dynamic part average testing (DPAT) [7] and nearest neighbor residual (NNR) [8],

[9] are widely used testing methods. DPAT is based on wafer-wide distribution and hence cannot capture the chips whose characteristics deviate significantly from the spatial trend. NNR, on the other hand, takes into account the local trend changes. It predicts the trend based on the characteristics of neighboring chips. However, since the prediction is carried out using the limited number of neighboring chips, the trend may be biased by the presence of a cluster of outliers.

In this study, adaptive detection of outlier chips based on a statistical methodology is proposed. The Gaussian process regression (GPR) [10], [11] with Student-t likelihood [12] is utilized to define both the spatial characteristic trend and the allowable range of the characteristic. GPR is a non-parametric statistical model that can calculate the underlying trends from the measured data without prior assumption of the model function. Through GPR, the credible interval can be obtained in addition to the mean of the prediction. Since this interval is an indicator for finding a statistically reasonable range of the chip characteristics, we use the interval to judge the outliers.

The proposed outlier detection method is validated using the wafer measurements of a commercial power MOSFET and an artificially generated dataset that we know the ground truth. The performance of the detection is compared with that of conventional methods. The experimental results show that the accuracy of the proposed method is significantly better than that of the conventional methods.

II. GAUSSIAN PROCESS REGRESSION

In this section, the details of Gaussian process regression (GPR) are explained. GPR is a regression method based on the Gaussian process and can be adapted without assuming the form of the regression function beforehand. From the known input-output pairs $\mathbf{X} \rightarrow \mathbf{Y}$ of a latent function f , the output Y^* that corresponds to arbitrary inputs X^* can be predicted using GPR. In GPR, the prediction Y^* is obtained as a probability distribution, which is useful for determining whether the regression results are credible or not. The narrower the distribution as a prediction, the greater the certainty, whereas the wider the distribution, the greater the likelihood that the actual observation may contain larger randomness.

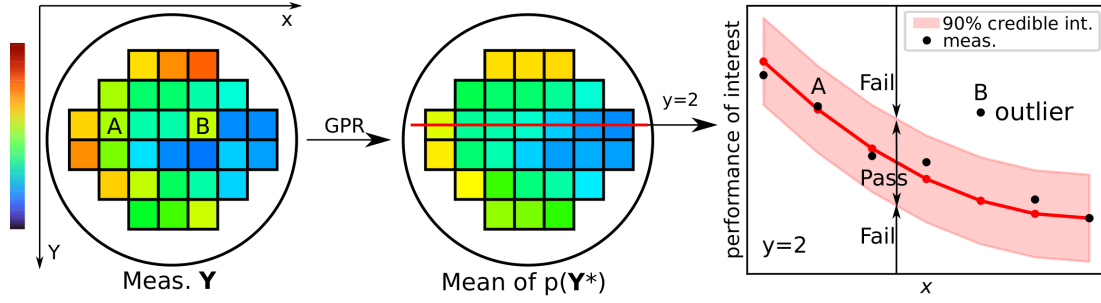


Fig. 1: Concept of the proposed adaptive outlier detection.

Assume that $\mathbf{f} = (f(X_1), f(X_2), \dots, f(X_n))$ as a set of random variables for inputs $\mathbf{X} = (X_1, X_2, \dots, X_n)$. When \mathbf{f} is a Gaussian process (GP), any finite subset follows a multivariate Gaussian distribution $p(\mathbf{f}) = \mathcal{N}(\boldsymbol{\mu}, \mathbf{K})$. Generally, the mean $\boldsymbol{\mu}$ is set to $\mathbf{0}$ and the covariance matrix $\mathbf{K} = (k_{ij})$ is calculated by a kernel function of \mathbf{X} . A typical kernel function is automatic relevance detection radial basis function (ARD-RBF):

$$k_{ij} = k(X_i, X_j) = \theta_1 \exp\left(-\sum_p \frac{|X_i^{(p)} - X_j^{(p)}|^2}{\theta_2^{(p)}}\right) \quad (1)$$

where p indicates each dimension of X . θ_1, θ_2 are hyperparameters. A set of observation \mathbf{Y} contains random noise in addition to \mathbf{f} . In case that the random noise follows the Student-t distribution,

$$\begin{aligned} p(Y_i|f_i) &= \mathcal{ST}(f_i, \nu, \sigma) \\ &= \frac{\Gamma((\nu+1)/2)}{\Gamma(\nu/2)\sqrt{\nu}\pi\sigma} \left(1 + \frac{(Y_i - f_i)^2}{\nu\sigma^2}\right)^{-(\nu+1)/2} \end{aligned} \quad (2)$$

where ν is called the degrees of freedom and σ the scale parameter. Since the Student-t distribution has heavier tails compared to the Gaussian distribution, it is tolerant to outliers. Specifically, GPR with Student-t noise is more robust against the outliers compared to that with Gaussian noise [12]. This property is important to ensure that the regression results are not overly influenced by outliers.

In order to deal with Student-t distribution, Laplace approximation is introduced.

$$p(\mathbf{f}|\mathbf{Y}) \approx \mathcal{N}(\hat{\mathbf{f}}|\boldsymbol{\Sigma}) \quad (3)$$

$$\hat{\mathbf{f}} = \operatorname{argmax}_{\mathbf{f}} p(\mathbf{f}|\mathbf{Y}) \quad (4)$$

$$\boldsymbol{\Sigma} = \mathbf{K}^{-1} + \mathbf{W} \quad (5)$$

$$\mathbf{W}_{ij} = \begin{cases} -(\nu+1) \frac{(Y_i - f_i)^2 - \nu\sigma^2}{((Y_i - f_i)^2 + \nu\sigma^2)^2} & (i=j) \\ 0 & (i \neq j) \end{cases} \quad (6)$$

All hyperparameters $\boldsymbol{\theta} = (\theta_1, \theta_2, \nu, \sigma)$ are optimized by maximizing log likelihood function \mathcal{L} [12].

$$\begin{aligned} \mathcal{L} &= \log p(\mathbf{Y}|\mathbf{X}, \boldsymbol{\theta}) \\ &= \log p(\mathbf{Y}|\hat{\mathbf{f}}) - \frac{1}{2} \log |\mathbf{K}| - \frac{1}{2} \hat{\mathbf{f}}^T \mathbf{K}^{-1} \hat{\mathbf{f}} \end{aligned} \quad (7)$$

$$- \frac{1}{2} \log |\mathbf{K}^{-1} + \mathbf{W}| \quad (8)$$

In practice, gradient-based methods, such as L-BFGS-B method, can be applied for the optimization.

The posterior distribution $p(f^*|X^*)$ for an arbitrary input X^* can be predicted as Gaussian distribution, because the concatenated vector $(\hat{\mathbf{f}}, f^*)$ also follows Gaussian process [12].

$$p\left(\begin{pmatrix} \hat{\mathbf{f}} \\ f^* \end{pmatrix}\right) = \mathcal{N}\left(\mathbf{0}, \begin{pmatrix} \mathbf{K} & \mathbf{K}_* \\ \mathbf{K}_*^T & k_{**} \end{pmatrix}\right) \quad (9)$$

$$p(f^*|\mathbf{X}^*, \mathbf{X}, \hat{\mathbf{f}}) = \mathcal{N}(\mathbf{K}_*^T \mathbf{K}^{-1} \hat{\mathbf{f}}, k_{**} - \mathbf{k}_*^T \mathbf{K}^{-1} \mathbf{k}_*) \quad (10)$$

where $\mathbf{K}_{*,i} = k(X_i, X^*)$, $k_{**} = k(X^*, X^*)$. Then, the prediction of the observation $p(Y^*)$ can be obtained by integrating Student-t distribution, which can be calculated by quadrature integration.

$$p(Y^*) = \int p(Y^*|f^*)p(f^*|\mathbf{X}^*, \mathbf{X}, \hat{\mathbf{f}})df^* \quad (11)$$

For implementing the proposed method, GPy [13], a Python library of Gaussian process, is used.

III. PROPOSED METHOD

In this section, a method for detecting outliers using GPR with Student-t noise is proposed. As described in the previous section, GPR is a Bayesian non-parametric regression method that yields a latent function with noise as a probability density. The Student-t noise is included to alleviate the effects of outliers, i.e., to avoid overfitting as compared to using standard Gaussian noise. In the proposed method, the spatial underlying trend of chip characteristics is considered as a latent function f , whose input X is the coordinate (x, y) of a chip and whose output with noise Y is the characteristics of that chip.

The concept of the proposed method is illustrated in Fig. 1. The measured value \mathbf{Y} of chips in a wafer follows an underlying spatial trend with some noise. GPR is applied to chip coordinate \mathbf{X} and the measured values \mathbf{Y} , to optimize the hyperparameters. Then, the posterior distribution $p(\mathbf{Y}^*)$ for each chip coordinate \mathbf{X}^* is predicted by GPR. Note that the mean of the distribution $p(\mathbf{Y}^*)$ is just one of the representations of the underlying trend, because the underlying trend is a set of distributions $p(\mathbf{f}^*)$. The probability of measured value to be in that distribution means the credibility of each chip on the basis of the underlying characteristics trend. From the set of posterior distribution $p(\mathbf{Y}^*)$, the $100(1-\alpha)\%$ credible interval can be calculated. Here, α is called rejection rate.

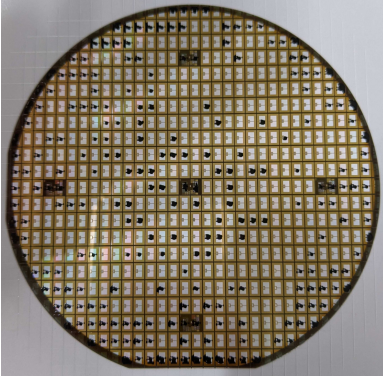


Fig. 2: Measured wafer of a commercial SiC MOSFET.

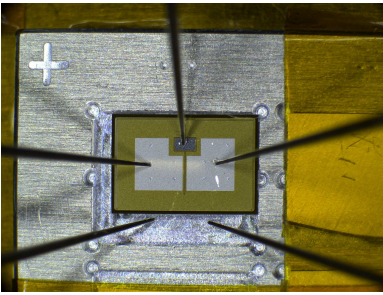


Fig. 3: Chip under measurement on an aluminum chip holder.

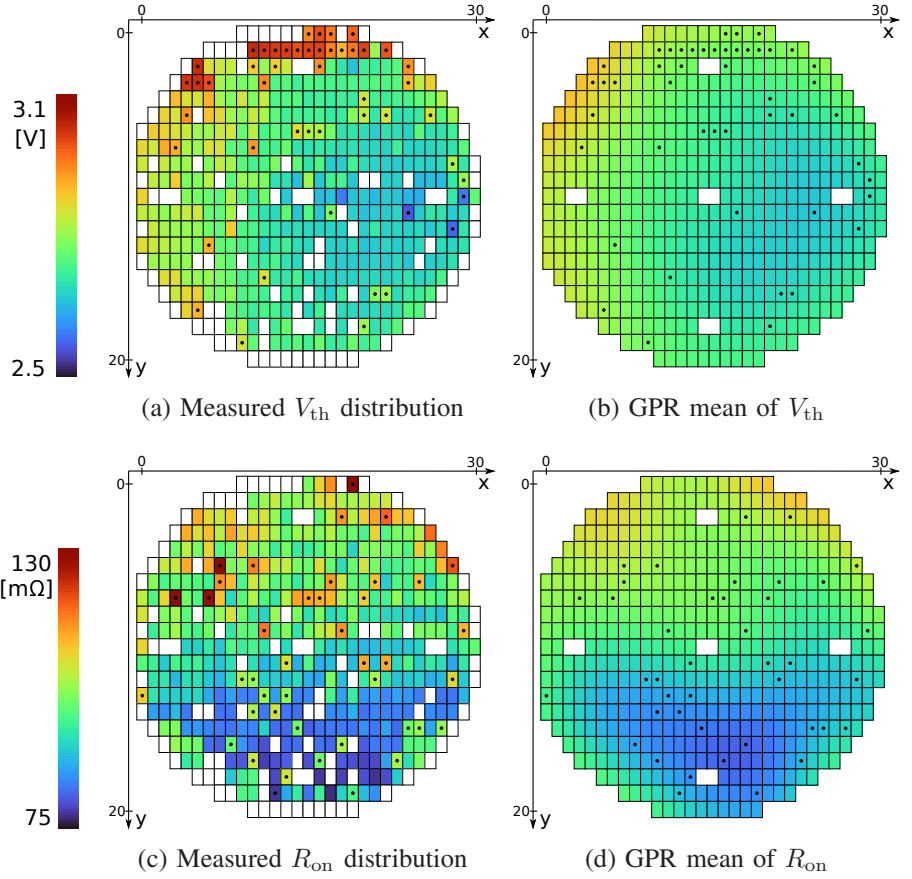


Fig. 4: Wafer measurement results and the underlying trend obtained as GPR mean. The chips with a dot are the outliers judged by the proposed method.

In the proposed method, the credible interval is used for the outlier detection. By comparing the measured values with their credible intervals, each chip is classified as either outlier or not. Fig. 1 shows an example wherein α is set as 0.1. Though the performances of chip A and chip B are close, chip B should be considered as an outlier while chip A is not, because the performance of chip B excessively deviates from the underlying trend. Chips like B are considered to potentially contain defects. By adaptively determining the test limit for each chip on the basis of the credible interval, the proposed method provides the optimal testing criteria even when the large underlying trend is expected.

More formally, the proposed outlier detection method consists of the following five steps.

- 1) Measure the performance of interest, such as on-resistance, breakdown voltage, threshold voltage, etc., of all available chips on a wafer.
- 2) Using the coordinates of chips \mathbf{X} and their measured characteristics \mathbf{Y} , the hyperparameters of GPR are optimized.
- 3) For the i -th chip in the wafer, infer by GPR the probability distribution of $p(Y_i^*)$ that Y_i should follow, with the chip coordinate X_i as X_i^*
- 4) Judge the chip as an outlier if Y_i is out of a $100(1 -$

$\alpha)$ % credible interval. Otherwise, the chip is considered consistent with the underlying trend.

- 5) When there exist multiple performances of interest, the rejection results are OR-ed. In other words, a chip that is judged to be an outlier in at least one performance should be considered as an outlier.

IV. MEASUREMENTS AND VALIDATION

In this section, the proposed method is validated and compared with the two conventional methods, DPAT and NNR. The results for the measurement data of a commercial SiC wafer are presented in Sec. IV-A, and the results of an artificially generated demo dataset are presented in Sec. IV-B.

A. Measurement of commercial wafer

The 435 chips on a commercial SiC wafer shown in Fig. 2 are measured. The photograph of a chip during probing is shown in Fig. 3. In this study, the threshold voltage V_{th} and on-resistance R_{on} are chosen as the performances of interest. V_{th} is defined as the gate voltage when $V_{ds} = 20$ V, $I_d = 4.4$ mA, and R_{on} is measured at $V_{gs} = 20$ V, $V_{ds} = 0.5$ V. The temperature of the wafer is controlled at 40°C .

Figs. 4(a) and 4(c) show the measured V_{th} and R_{on} distributions. The measured values of V_{th} range from 2.5 to 3.1 V,

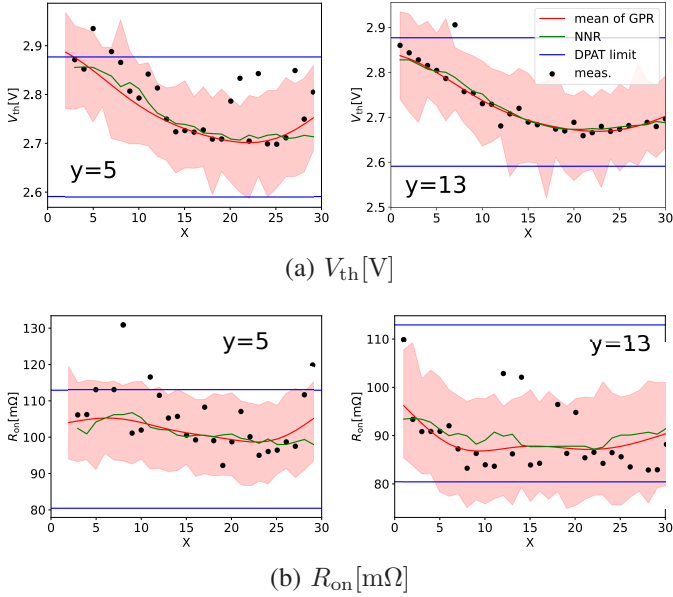


Fig. 5: Measurement versus the mean of GPR with 90% credible interval at $y = 5$ and $y = 13$. The trend given by NNR and the thresholds given by DPAT are also drawn.

and those of R_{on} range from 75 to 130 mΩ. Most of these values are still within the range of the official datasheet. However, chips having the values significantly off the underlying trend present randomly on the wafer. In other words, those devices that exhibit significantly different characteristics from their surrounding trend can be considered to have long-term reliability issues. The means of GPR posterior distribution are shown in Fig. 4(b) for V_{th} and Fig. 4(d) for R_{on} . Here, the GPR posterior prediction is considered as the underlying trend, and regard the chips with their measured value exceeding 90% credible interval as outliers. The detected outliers for each performance are marked with a black dot in Fig. 4. From the figure, it can be said that the proposed method successfully detects outlier chips. It is found that V_{th} follows the estimated underlying trend well, while R_{on} suffers from a larger random component. As a result, there are as many outliers in V_{th} as those in R_{on} , because the prediction of V_{th} has a narrower credible interval.

Fig. 5 shows a comparison of the measurement and the predicted distributions of GPR for the rows $y = 5$ and 13 . In these figures, in addition to the mean of the estimated distribution, the 90% credible intervals are also depicted. Regarding V_{th} of $y = 13$, most of the chips are located very close to the estimated mean curve and have fallen within the credible interval, indicating the underlying trend is dominant over random noise. R_{on} of $y = 5$ has a wider credible interval due to the large random noise. Meanwhile, though there are many outliers for V_{th} of $y = 5$ and R_{on} of $y = 13$, the GPR posterior is not overfitted to them.

The 90% (1.645σ) limit of DPAT and the underlying trend predicted by NNR are also indicated in Fig. 5. Since DPAT imposes the same limit for all the chips without taking into

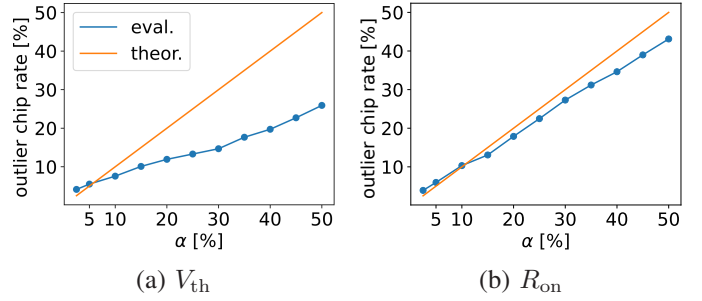


Fig. 6: The relationship between α and outlier chip rate. The theoretical line where α is equal to the outlier chip rate is also drawn.

account the underlying trends on the wafer, a large number of outlier chips with different characteristics from their neighbors are classified as inliers. This may lead to inappropriate testing results. The NNR trend is not smooth compared to the GPR mean. Since the residual from the NNR trend is often utilized to judge outliers, the unsmooth trend may cause wrong judgments.

In the proposed method, the fraction of chips that are judged as outliers is highly dependent on the rejection rate α . In order to reject potential outliers close to the threshold, a larger α may be used. However, too large α value will result in a lower yield, so it must be set carefully. Fig. 6 shows the outlier chip rate as a function of α . Here, the outlier chip rate is defined as the ratio of chips that are determined to be outliers out of all chips measured.

When α is small, the outlier chip rate becomes higher than what is expected by α because there exist significantly bad performing chips that will be judged outliers regardless of the value of α . In contrast, when α is larger than 0.2, the outlier chip rate is less than what is expected by α . In that range of α , less obvious outliers are found, resulting in more yield loss. Therefore, the intersection where α becomes equal to the outlier rate can be used as a good candidate to determine the appropriate α value. In this example, α is defined at around 0.1 for both V_{th} and R_{on} characteristics.

B. Virtual measurement dataset

In order to demonstrate the effectiveness of the proposed method, a virtual dataset consisting of 519 chips on a wafer shown in Fig. 7(a) is generated. The virtual performance data $p(x, y)$ has a baseline trend that consists of two components: global variation component $p_g(x, y)$ as a function of the chip coordinate (x, y) on the wafer and random variation component p_r that is sampled from a normal distribution that is mutually independent and identical for each chip. Here, the coordinates x and y are both integers. Additionally, a relatively large random deviation p_d was taken into account for the 20% of the entire chips. The chips with this extra component added are defective and thus should be judged as outliers. The overall performance of a chip is determined by:

$$p(x, y) = p_g(x, y) + p_r + p_d, \quad (12)$$

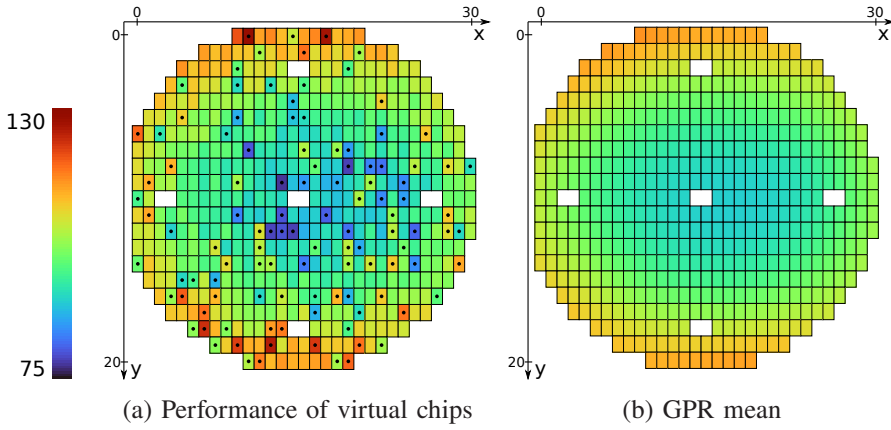


Fig. 7: Visualization of a virtual measurement dataset. The chips with a dot are the outliers determined by the proposed method.

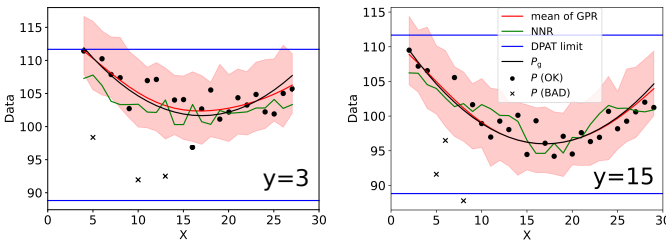


Fig. 9: Virtual measurement data versus the mean of GPR with 80% credible interval at $y = 3$ and $y = 15$. The trend given by NNR and the thresholds given by DPAT are also drawn.

where

$$p_g(x, y) = 90 + 0.06((x - 17)^2 + 4(y - 11)^2) \quad (13)$$

$$p_r \stackrel{iid}{\sim} \mathcal{N}(2.0, 1.0) \quad (14)$$

$$p_d \stackrel{iid}{\sim} \begin{cases} 0 & (80\%) \\ \text{Uniform}(9, 11) & (10\%) \\ \text{Uniform}(-11, -9) & (10\%) \end{cases} \quad (15)$$

Fig. 7(b) shows the mean of the GPR posterior distribution. The global trend given by Eq. (13) is reproduced by the proposed method. The theoretical and GPR-based outlier chip rates as functions of α are shown in Fig. 8. From the intersection in Fig. 8, the α is set to 0.2. In Fig. 9, the virtual data along $y = 3$ and $y = 15$ is presented with the mean and the credible interval of the GPR. Even with the presence of outliers, the proposed method extracts reasonably smooth global trend, which is very close to the true global variation p_g , and provides a reasonable threshold for separating good chips from defective ones. The given chips with different performance components are classified properly. In contrast, the threshold given by the DPAT is too broad and most of the outlier chips have fallen in the “pass” region. Similarly, the background trend extracted by the NNR method is different from the ground truth due to the influence of outliers.

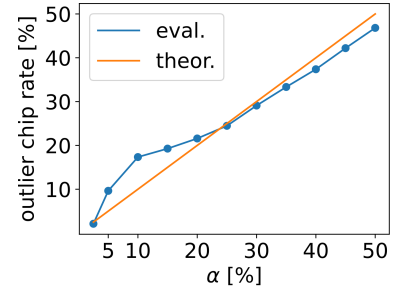


Fig. 8: The relationship between α and the outlier chip rate for the virtual measurement dataset. The theoretical line where α is equal to the outlier chip rate is also drawn.

The accuracy of each outlier detection method is evaluated for the virtual wafer in Fig. 7 and summarized in Table I. The components of the confusion matrix given by each method, sensitivity, and specificity are presented. In terms of confusion matrix, the proposed method clearly outperforms the two existing methods. Accordingly, the sensitivity and specificity of the proposed method are better than that of NNR and DPAT. In particular, the sensitivity of the proposed method is 1.00, meaning that all the given outliers are detected. The specificity is 0.98, which means that the rate of misclassification of inliers as outliers is remarkably small.

V. CONCLUSION

In this study, an adaptive outlier detection methodology based on the predicted posterior of GPR is proposed. The proposed method successfully detected outliers in both experiments using the measurement data of a commercial SiC wafer and virtual measurement dataset. In the experiments using the virtual measurement data, the accuracy of the proposed method significantly outperformed the two conventional methods, NNR and DPAT. Though V_{th} and R_{on} are selected as the performance of interests, the proposed method can be effective for the tests using other characteristics, such as breakdown voltage or parasitic capacitances.

ACKNOWLEDGMENT

The part of this work is supported by JST-OPERA Program Grant Number JPMJOP1841, JSPS KAKENHI Grant 20H04156, and 20K21793.

REFERENCES

- [1] B. Stine, D. Boning, and J. Chung, “Analysis and decomposition of spatial variation in integrated circuit processes and devices,” *IEEE Transactions on Semiconductor Manufacturing*, vol. 10, no. 1, pp. 24–41, Feb. 1997.
- [2] T. Kimoto, “Bulk and epitaxial growth of silicon carbide,” *Progress in Crystal Growth and Characterization of Materials*, vol. 62, no. 2, pp. 329–351, Jun. 2016.
- [3] Y. Cui, X. Hu, X. Xie, R. Wang, and X. Xu, “Spatial variation of lattice plane bending of 4H-SiC substrates,” *CrystEngComm*, vol. 19, no. 27, pp. 3844–3849, 2017.

TABLE I: Accuracy comparison of outlier detection methods. Positive and negative refer to outliers and inliers, respectively. Sensitivity is the rate of outliers detected out of all given outliers. Specificity is the rate of inliers detected out of all given inliers. Higher score is better for both sensitivity and specificity.

Method	True Positive	True Negative	False Positive (yield loss)	False Negative (test escape)	Sensitivity	Specificity
This work	102	407	10	0	1.00	0.98
NNR	89	395	22	13	0.87	0.95
DPAT	44	384	33	58	0.43	0.92

- [4] N. A. Mahadik, H. Das, S. Stoupin, R. E. Stahlbush, P. L. Bonanno, X. Xu, V. Rengarajan, and G. E. Ruland, "Evolution of lattice distortions in 4H-SiC wafers with varying doping," *Scientific Reports*, vol. 10, no. 1, p. 10845, Jul. 2020.
- [5] K. Hasegawa, K. Taguchi, Y. Kagawa, E. Suekawa, N. Kaguchi, Y. Ata, H. Haruguchi, Y. Nakashima, and T. Minato, "Which is harder SOA test for SiC MOSFET to do Unclamped Inductive Switching (UIS) or Unloaded Short Circuit mode switching (USCS)? Does UIS play a role of USCS?" in *Proceedings of International Symposium on Power Semiconductor Devices and ICs (ISPSD)*, Sep. 2020, pp. 62–65.
- [6] R. Madge, M. Rehani, K. Cota, and W. Daasch, "Statistical post-processing at wafersort — an alternative to burn-in and a manufacturable solution to test limit setting for sub-micron technologies," in *Proceedings of IEEE VLSI Test Symposium (VTS)*, Apr. 2002, pp. 69–74.
- [7] *Guidelines for part average testing*, Automotive Electronics Council (AEC), 2011. [Online]. Available: http://www.aecouncil.com/Documents/AEC_Q001_Rev_D.pdf
- [8] W. Daasch, J. McNames, D. Bockelman, and K. Cota, "Variance reduction using wafer patterns in I_{DDQ} data," in *Proceedings of International Test Conference (ITS)*, Oct. 2000, pp. 189–198.
- [9] S. Sabade and D. Walker, "Comparison of wafer-level spatial I_{DDQ} estimation methods: NNR versus NCR," in *Proceedings of IEEE International Workshop on Current and Defect Based Testing (DBT)*, Apr. 2004, pp. 17–22.
- [10] C. E. Rasmussen and C. K. I. Williams, *Gaussian Processes for Machine Learning*, ser. Adaptive Computation and Machine Learning series, F. Bach, Ed. Cambridge, MA, USA: MIT Press, Nov. 2005.
- [11] C. Bishop, *Pattern Recognition and Machine Learning*, ser. Information Science and Statistics. New York: Springer-Verlag, 2006.
- [12] J. Vanhatalo, P. Jylänki, and A. Vehtari, "Gaussian process regression with Student-t likelihood," in *Proceedings of Advances in Neural Information Processing Systems (NeurIPS)*, vol. 22. Curran Associates, Inc., 2009.
- [13] GPpy, "GPpy: A gaussian process framework in python," <http://github.com/SheffieldML/GPy>, since 2012.